In situ scanning-tunneling-microscopy studies of early-stage electromigration in Ag

L. E. Levine,* G. Reiss,† and D. A. Smith‡
IBM Research Division, Thomas J. Watson Research Center, Yorktown Heights, New York 10598
(Received 14 December 1992)

The mass-transport mechanisms that are responsible for the early stages (resistance change $<1\%$) of electromigration damage in metals are poorly understood. A deeper understanding of these processes is important both for the direct application to metal lines in electronic devices and for expanding our basic knowledge of these complex phenomena. A major reason for our lack of understanding is that the structural changes that must take place during early-stage electromigration occur at extremely small length scales that are beyond the resolution capabilities of conventional electromigration experiments. We report *in situ* studies of early-stage electromigration using scanning tunneling microscopy. A single 2-μm square region of a 2100-Å Ag film was studied under UHV conditions for over 200 h with current densities up to 4.5×10^4 A/cm^2. Although the temperature and resistivity of the sample remained nearly constant throughout this period, significant small-scale morphology changes occurred that were a result of the applied current.

INTRODUCTION

Annealing treatments and high current densities can often cause structural changes in polycrystalline metallic films. In the case of annealing, these modifications are due to the minimization of the surface and grain boundary energies of the film material and depend additionally on the energy of the substrate/film interface. In current-carrying thin films, the electric field and the related flow of electrons create additional forces that result in a directed flow of material (electromigration). This mass transport, along with thermal gradients, causes stress gradients in the films which can counteract or enhance the migration of the material. Other factors that must be taken into account include three different diffusivities (bulk, grain boundary, and surface), the sizes and orientations of the grains, the dimensions of the investigated structures, and the role of second phase precipitates. Factors such as local inhomogeneities of the electric field may also play an important role in this process. The relative importance of these many factors varies for different materials and for different temperature and current density regimes. For recent reviews of these related problems see, for example, the discussions given by Ho and Kwok[1] or Scorzoni *et al.*[2]

Since all of the above factors apply to phenomena which are operative on very small length scales, microscopic studies of the structural changes that occur during heat or current treatment and therefore important for the basic understanding of the related physics as well as for the application to thin films and lines in electronic devices. To date, most of the experimental work on electromigration has used a combination of statistical median time to failure (MTF) analysis with subsequent *ex situ* scanning electron microscopy (SEM) or transmission electron microscopy (TEM).[3,4] Only a small number of publications reported microscopic *in situ* studies of electromigration with the SEM (Ref. 5) or TEM.[6] *In situ* microscopic studies, however, allow continuous monitoring of the electromigration process and promise to provide new insights into the observed structural modifications.

SEM and scanning tunneling microscopy (STM) seem to be especially appropriate for this purpose. The established *in situ* SEM technique offers both large-scale and microscopic imaging with a resolution down to about 10 nm. *In situ* STM gives the opportunity of imaging the surfaces with a resolution down to 0.2 nm and provides quantitative height profiles. Until now, however, there are no published reports of *in situ* STM studies of electromigration in thin metal films. We are in communication with Paniccia, Flinn, and Reifenberger, however, who are currently working on in-air STM studies of electromigration in Au films.[7]

The high resolution of a STM is particularly promising for studying the early stages of electromigration. Such studies would allow microscopic examination of the electromigration-induced changes that are expected to occur at temperatures and current densities lower than those used in more conventional accelerated experiments. To date, early-stage electromigration studies have concentrated on measuring minute variations in electrical resistance, $\Delta R/R_0$, or on measuring low-frequency noise in metal lines. Such measurements are then compared theoretically to various hypothesized structural changes within the line.[2,8] A direct comparison to measured structural changes is clearly preferable. One landmark SEM study did count the number of visible voids and cracks in four samples as a function of sample resistance;[9] most of the data were taken in the resistance range $1\% \le \Delta R/R_0 \le 10\%$. As we shall demonstrate in this paper, however, the dramatically higher resolution of the STM allows observation of much finer detail at even lower values of $\Delta R/R_0$.

As previously reported, we have constructed an UHV STM system capable of studying annealing and electromigration processes *in situ* on heated, current-carrying thin films.[10] The STM system is constructed to allow coarse motion of at least 5 mm/axis on all three axes. Such con-

0163-1829/93/48(2)/858(6)/$06.00

trol is used to locate interesting regions of the sample and to compensate for drifts experienced during sample heating. The system uses a potentiometric STM design which overcomes the problem of decoupling the STM electronics from the dc voltage drop over a current-carrying sample. The design involves a Wheatstone bridge arrangement and a feedback responding only to selected ac components of the tunneling current. The potentiometric capabilities should also allow direct imaging of voltage drops across microscopic features such as grain boundaries and second phase precipitates.[10–12]

In this paper we present the results of an *in situ* topographic STM study of early stage electromigration in a Ag film using this STM system. We define the early-stage electromigration regime as the time and current density range in which the sample resistance remains constant to within 1% of the initial value. For the time scale of this experiment, this range included current densities up to 5.0×10^4 A/cm^2. Joule heating of the Ag film at this current density caused a temperature increase of only 4 °C.

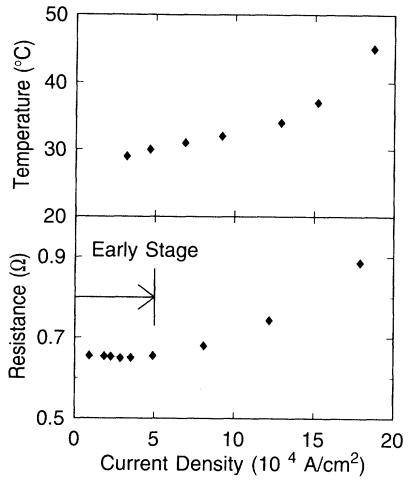

FIG. 1. Temperature and resistance calibration curves for our 2100-Å Ag film samples.

PREPARATION AND CHARACTERIZATION OF SAMPLES

Our Ag films were produced by evaporation onto room-temperature mica substrates at a rate of 2 Å/sec with a base pressure of 9×10^{-8} Torr. The film thickness was 2100 Å. Auger depth profiling showed no detectable sample contamination below the first 40 Å. Atomic detection limits were $<1\%$. The sample surface showed high initial oxygen contamination that decreased to nearly a monolayer after three days in UHV. Other significant surface contaminants included Cl ($\approx10\%$), C, and S. The C Auger energy was superimposed on a Ag signal, making quantitative analysis questionable. We estimate the C contamination to be roughly equal to the Cl contamination. The S contamination was significantly lower, in the range of a few percent. Data were taken from a 25-μm^2 area, thus averaging over both grains and grain boundaries.

Sample resistance and temperature as a function of current density were measured in a separate vacuum chamber for multiple identical samples. Sample current was increased slowly for these measurements over a period of many days until sample failure. Postfailure SEM studies were carried out on all electromigration samples and showed the same thermal-runaway failure mechanism. The film temperature was measured using a small mass thermocouple in contact with the film surface. Resistance was measured using a quasi-four-point-probe arrangement. All resistance and temperature measurements were consistent. Representative curves for the early electromigration regime are shown in Fig. 1.

As-deposited Ag films were examined in a Philips 430 TEM with a beam voltage of 300 kV. Microdiffraction, selected area diffraction, and real space imaging were used to determine grain sizes and orientations. Results show the film to be weakly (111) textured with a roughly bimodal grain size distribution containing large grains ≈250 nm across and many smaller grains <100 nm wide. Some of these smaller grains overlap other grains. Occasional grains that are 0.7–1.0 μm across also occur; at least some of these grains are (111) textured and are lattice aligned with the mica substrate. These details are in agreement with previously published STM images of Ag on mica grown under comparable conditions[13] and with the STM data from our own as-deposited samples. We conclude that the apparent grain structure visible in the STM corresponds to actual grains with small-scale grain boundary grooving. A separate publication[14] to discuss this topic in greater detail is planned.

EXPERIMENTAL PROCEDURE

The Ag samples examined in the UHV STM measured 5 mm between the electrical contacts and were 1.5 mm wide. The samples were studied at a base pressure of 1×10^{-10} Torr. The partial pressure of O_2 was in the 10^{-13}-Torr range, which is many orders of magnitude below the room-temperature decomposition pressure for Ag_2O ($\approx10^{-3}$ Torr). We started STM tunneling after an initial waiting period of several days; the tunneling current was extremely stable, indicating that any residual oxide layer was minimal. This behavior is in agreement with the Auger results discussed earlier.

Two separate samples were studied using the same experimental procedure. The first sample was used primarily as a test case to prepare for a more in-depth study on the second sample. The results from both experiments were consistent and we will primarily concentrate on results from the second electromigration sample. During the *in situ* electromigration studies, our procedure was to increase the dc sample current by a few mA and take repeated scans of one general area for several hours. Current was applied using a constant current source. Scan sizes ranged from 2.0 μm down to 0.1 μm square. If no significant changes were observed, the sample current was again increased. During the second run, this procedure continued for 256 h until the sample failed at a

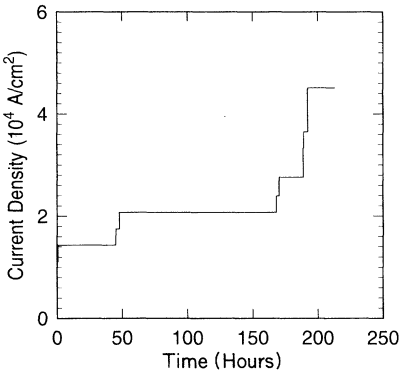

FIG. 2. Applied dc current density as a function of time for our second electromigration experiment on Ag films.

current density of 3.2×10^5 A/cm^2. For most of this time, $\Delta R/R_0$ remained constant to within $<1\%$. Figure 2 shows the dc sample current as a function of time for the early electromigration stage of our second run. During this period, 292 scans were taken from the sample. We compensated for sample drift and stayed centered over the same 2-μm square area of the sample throughout the experiment.

In order to separate the effects of annealing and current flow, we also completed an *in situ* STM study on an indirectly heated Ag film. A maximum temperature of 140 °C was reached after 391 h. This temperature far exceeded the highest temperature reached during our study of the early stages of electromigration. None of the structural changes reported in this paper were observed in the indirectly heated sample.

All of the STM images displayed in this paper were obtained from 750-nm square topographic scans composed of 256×256 data points. A plane was subtracted from the data and no other image processing algorithms were used. The ac bias voltage was 300 mV and the ac tunneling current was 10 nA. The tunneling tip was produced from a 0.5-mm electrochemically etched tungsten wire. SEM studies of identically prepared tips showed them to have a radius of ≤ 50 nm.

In this paper we discuss the various driving forces present in our samples and relate them to the structural modifications we observed during the early stages of electromigration. As previously mentioned, this includes all changes up to a current density of 5.0×10^4 A/cm^2. The structural modifications that occurred in later stages were fundamentally different and we plan to discuss them in a separate publication.[15]

DRIVING FORCES

The primary driving forces that can bias atomic motion in metal films are electrical, thermal, and mechanical in nature. Electromigration results from the electrical driving force and is usually described by the expression

$$\mathbf{F}=Z^*e\mathbf{E}=Z^*e\rho\mathbf{j}\ ,$$

where $\mathbf{E}$ is the electrostatic field, ρ is the resistivity of the metal, $\mathbf{j}$ is the local current, and Z^* is the effective charge number.[2] Substituting in for the resistivity of Ag and the approximate value[1] of $Z^*=-8$ gives

$$\mathbf{F}=\mathbf{j}(1.3\times10^{-3})\ \text{eV/m}\ ,$$

where $\mathbf{j}$ is in units of A/cm^2. The maximum electromigration driving force during the early stage of our experiment was thus 57 eV/m.

The driving force resulting from thermal gradients is described by the equation

$$\mathbf{F}=-Q^*\frac{\nabla T}{T}\ ,$$

where Q^* is the heat of transport and equals the energy flow per unit mass transported minus the intrinsic heat of solution.[16] Experimental measurements for Q^* in the literature are inconsistent for most metals. Using an extreme upper bound estimate of 0.5 eV for Q^* (Q^* for Al is 0.03 eV) and 2.5 K/mm for the maximum value for our thermal gradients at 306 K gives a maximum thermal driving force of 4 eV/m which is insignificant compared to the electromigration driving force.

The mechanical induced driving force has three primary components: the intrinsic process-induced stress field, the stress field produced by differing thermal expansions of the film and substrate during Joule heating, and the stress gradients induced by electromigration. Our Ag samples were produced by evaporation onto room-temperature mica substrates and were not subsequently annealed, thus limiting the intrinsic stress field. In addition, to a good approximation the intrinsic elastic stresses in the film are homogeneous and therefore do not lead to gradients which would be relaxed by material transport. As previously mentioned, additional *in situ* STM measurements were made on an indirectly heated Ag film. Sample temperatures of 140 °C were reached. Stress gradients were produced due to the differing thermal expansion coefficients of the film and substrate. These stress gradients were many times more severe than the gradients produced during the electromigration study. No significant topographical changes were observed in the annealing experiment, suggesting that the expansion-induced mechanical driving forces were insignificant for our early-stage electromigration experiment. The large stress gradients produced by electromigration in short lines result from mass flow into a confined volume and/or mass flow with restricted vacancy migration.[17] In experiments using uncapped lines, this confinement and vacancy barrier is provided by a rigid oxide layer. Since our samples have no confining layer, large-scale electromigration-induced stress gradients are not possible. Highly localized gradients in the region of structural changes, however, could still play a role in limiting the evolution of such changes but should have little effect in the early stages of their development.

RESULTS

The first significant change in our Ag sample was the appearance of small nodules, 24.6 h into the experiment,

at a current density of 1.4×10^4 A/cm^2. The nodules measured $\approx$350 Å in width and $<$30 Å in height and could not have been clearly resolved using conventional SEM techniques. The nodules are clearly mass concentrations since they are too small to be the result of film delamination.

The nodules grew at classic grain boundary divergence points such as triple junctions with just one grain boundary pointed roughly in the direction of the electron flux. Figure 3 shows a 0.75-μm scan taken at 46.2 h at a current density of 1.4×10^4 A/cm^2. The range of the height distribution for the scan is 300 Å (black-white). The small arrows mark representative nodules and the large arrow points in the direction of the electron flux. Figures 4(a) and 4(b) show line plots of the same area of the sample before and after the appearance of the nodules. The nodules grew to full size in $\approx$20 min and then decreased in size until they completely disappeared $\approx$60 h later. This behavior suggests the preferential removal of contaminants from the sample by surface diffusion along the grain boundaries to classic divergence points. The final size of the nodules is likely determined by a steady-state condition between the triple junction flux divergence and surface diffusion away from the nodule edges.

The nodule material is conductive and is most likely the C detected in the Auger analysis. If significant surface and grain boundary diffusion of the Ag were taking place, it would show up clearly as grain boundary grooving, which was observed at longer times and higher current densities. Our high resolution of $\approx$2 Å makes us very sensitive to such changes. Figure 5 shows height profiles for the area shown in Figs. 4(a) and 4(b). The similarity of the distributions demonstrates that no significant changes in grain boundary grooving took place between these two scans.

A typical nodule at a grain boundary triple point has a volume of 2×10^6 Å^3 and contains $\approx3\times10^5$ atoms, assuming C as the principal constituent. Using the initial

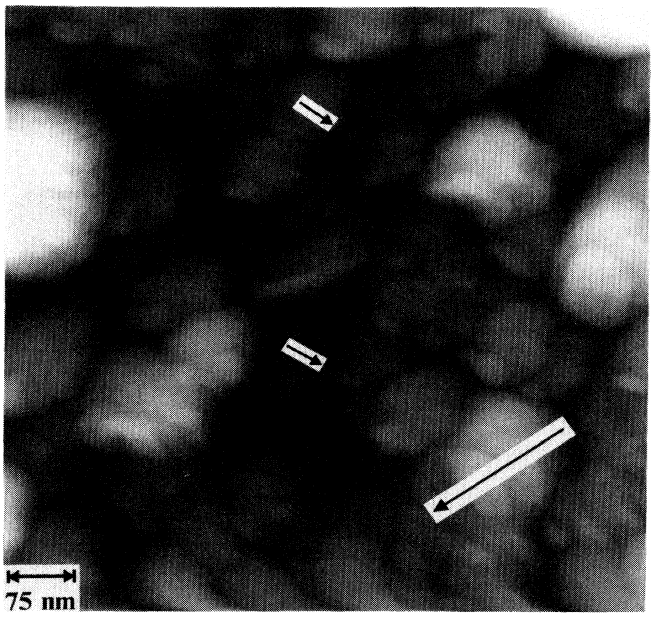

FIG. 3. Topographic STM scan of a Ag film carrying a dc current of 1.4×10^4 A/cm^2. The range of the height distribution for the scan is 300 Å (black-white). The small arrows indicate representative small nodules at divergence points and the large arrow points in the direction of the electron flux.

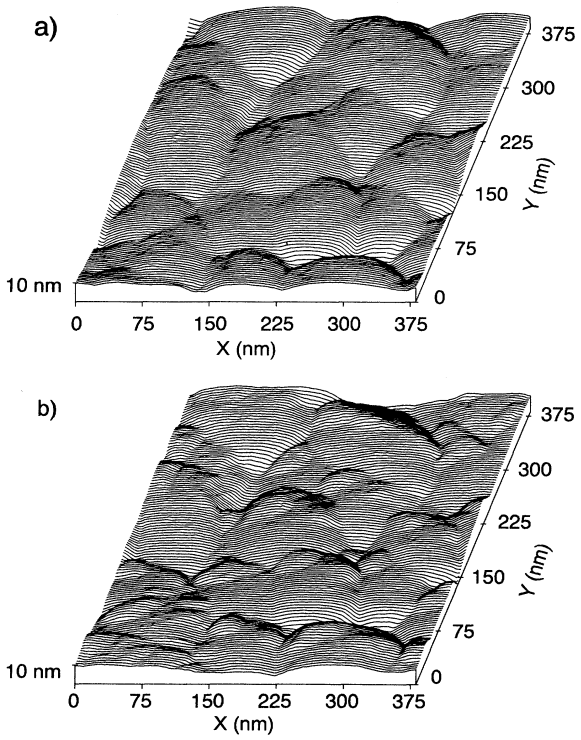

FIG. 4. Line plots of topographic STM scans of the same area as shown in Fig. 3 imaged (a) before and (b) after nodule formation.

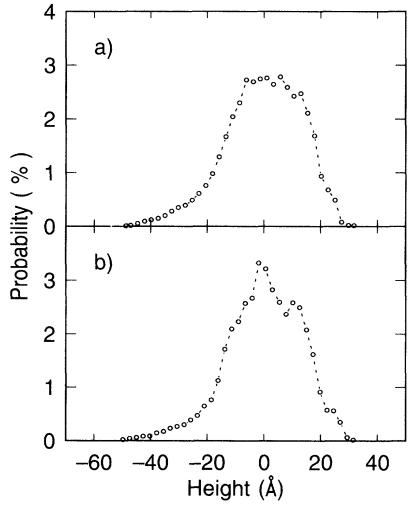

FIG. 5. Height profiles for the images in Fig. 4. The similarity of the distributions shows that no significant grain boundary grooving took place between these two scans.

growth rate to estimate the atomic flux divergence at the triple points gives $J_{div}=J_2+J_3-J_1=250$ atoms/sec. The nodule density on the sample is ≈ 100 nodules/μm^2. This accounts for ≈ 20 at. % of the top 20 Å of the sample where the majority of the sample contamination resides. This percentage is consistent with the suggestion that the nodules contain the bulk of the initial surface contamination which is eventually swept away toward the anode.

The second significant change that was observed in the sample was current-induced grain boundary grooving. As previously discussed, the degree of grain boundary grooving in our samples can best be quantified using height distribution profiles. Figure 6 shows two height profiles from the same 0.5-μm area of the sample; scans 6a and 6b were taken at 46.1 and 68.9 h, respectively. The current density during most of this period was 2.1×10^4 A/cm^2. The spreading of the height distribution is primarily due to a deepening and broadening of the grooves at the grain boundaries. Grain boundary grooving occurred very gradually throughout the experiment but was most pronounced during this period. This apparent slow down of the grain boundary grooving could be due, in part, to the inherent inability of our tip to penetrate and detect narrow crevices in the sample.

To understand the mechanism of current-induced grain boundary grooving in our sample, we must first examine conventional thermal-induced grooving. Thermal grooving may occur by three different mechanisms: evaporation/condensation, surface diffusion, or bulk vacancy migration to the boundary/surface intersection. The small temperature change in our experiment eliminates evaporation/condensation as a viable mechanism for our sample. Application of a current would have only a small effect on the bulk vacancy concentration and should only effect grain boundary grooving by increasing the rate at which the vacancies intersect the grain boundaries. This affect would result in increased grain boundary grooving for boundaries perpendicular to the current flow, an effect which was not observed. The most likely mechanism, therefore, is current driven surface diffusion in which the relatively unstable atoms at the grain boundary/surface intersection are perturbed out of their positions and preferentially migrate in the direction of the electron flux. A controlled experiment using bicrystals could investigate this phenomenon more closely by measuring cross sections of the grain boundary and comparing the overall shape to model calculations. Unlike grain boundary cross sections from thermal grooving, current grooved grain boundaries should be asymmetric. Unfortunately, the small size of our grains makes our Ag measurements unreliable for this purpose.

Another significant change observed in the sample strongly resembles classical thermally induced grain growth. Such growth was not observed, however, in our indirectly heated sample. Figure 7 shows four scans of the same region of the sample. The times and current densities for the four panels are (a) 82.8 h, 2.1×10^4 A/cm^2; (b) 99.8 h, 2.1×10^4 A/cm^2; (c) 101.8 h, 2.1×10^4 A/cm^2; and (d) 173.7 h, 2.8×10^4 A/cm^2. The range of the height distribution for the four scans is 360 Å (black-white). The sequence of scans shows a gradual transformation by migration of individual grain boundaries which culminates in the annihilation of a small grain. If this interpretation is correct, then the final grain configuration has lowered its energy by reducing its grain boundary area. Since the STM only probes the surface of a sample, we cannot say conclusively that the observed change extends into the bulk. It is possible that diffusing

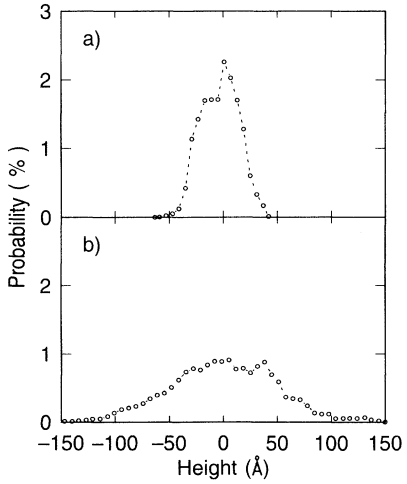

FIG. 6. Height profiles for images taken from the same area at 46.1 and 68.9 h. The redistribution in heights is mainly due to current-induced grain boundary grooving.

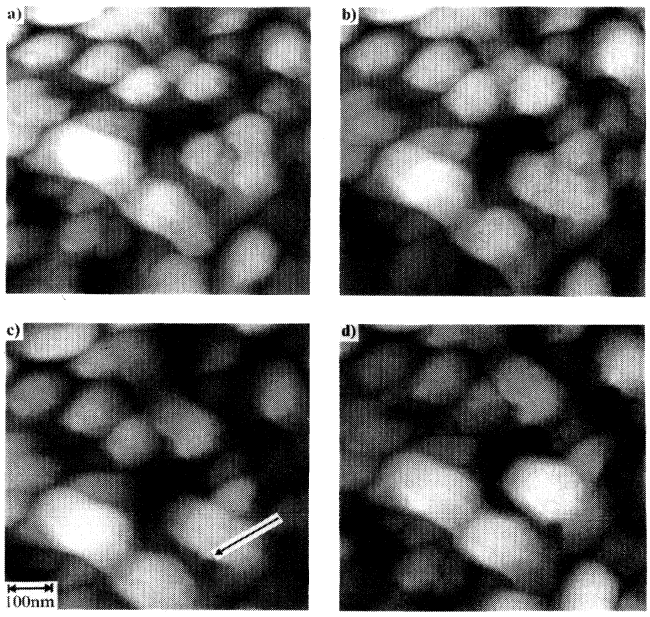

FIG. 7. Four topographic STM scans from the same area of the sample at different times and current densities as described in the text. The range for the height scale is 360 Å and the arrow points in the direction of the current flow. The structural changes suggest a grain growth mechanism driven by current transport.

adatoms preferentially adhered to one side of the intruding grain, causing an overgrowth of the marked grain. Evidence of such overgrowths appeared at much higher current densities and a separate publication discussing this and other late stage electromigration[14] effects is planned. These overgrowths, however, exhibited a strong correlation with the direction of current flow which is not seen in the structural changes shown in Fig. 6. We conclude that the transformation shown in Fig. 6 is most likely an example of grain growth driven by the current transport. This particular example was the only such occurrence observed within the 2-μm scan area. This suggests that the grain boundaries in this area of the film were either exceptionally mobile or subject to a locally higher driving force.

CONCLUSIONS

We have presented the results of the first *in situ* STM study of early-stage electromigration. We succeeded in obtaining extensive data from a single 2-μm square region of a Ag film for over 200 h while increasing the current density from 0.0 to 4.5×10^4 A/cm^2. During this period, our sample resistance remained constant to within $<1\%$. Nevertheless, significant structural changes were observed that, because of their small scale, could not have been resolved using any other available microscopic technique. These changes include the growth of small nodules at classic divergence points, current-induced grain boundary grooving, and a grain growth mechanism that strongly resembles classical thermally induced grain growth. We have shown that these phenomena are not thermally induced and that the electromigration force was dominant in this experiment.

A number of conclusions may be drawn from the above observations. First, the nodule growth demonstrates that mass can accumulate by surface diffusion to classic divergence points at extremely low current densities. Second, the observed grain growth mechanism shows that not all electromigration phenomena are destructive. This particular mechanism resulted in a more stable grain configuration that should possess a slightly lower electrical resistance due to the net decrease in grain boundary area. Third, the only structural change we observed in our sample that could account for a steady increase in sample resistance during the early stage of electromigration was current-induced grain boundary grooving. Clearly, the voltage drop across these grain boundaries should increase as the grooves deepen. This result provides direct observational support for earlier resistometric studies which suggested that extended aggregation of vacancies at the grain boundaries and grain boundary grooving were in large part responsible for resistance increases during early stage electromigration.[8] Grain boundary grooving should be significantly inhibited in capped structures by decreasing surface diffusion and limiting the availability of vacancies. Such effects could be simulated by evaporating 10–20 Å of Cr on top of our films. This type of procedure would still allow topographic STM studies and should work on metal lines as well as films. Finally, we remark that the current density at which we first observed destructive electromigration effects was substantially below the $\Delta R/R_0=1\%$ level often used to characterize early-stage electromigration.

We conclude that *in situ* STM studies hold great promise both for characterizing electromigration effects at the low temperatures and current densities found in real devices and for increasing our basic scientific understanding of such complex phenomena.

---

*Present address: Department of Physics, Washington University, St. Louis, Missouri 63130.
†Present address: IFW Dresden, Helmholtz Strasse, 0-8027 Dresden, Germany.
‡Present address: Department of Materials Science and Engineering, Stevens Institute of Technology, Castle Point on the Hudson, Hoboken, New Jersey 07030.

[1]P. S. Ho and T. Kwok, Rep. Prog. Phys. **52**, 301 (1989).
[2]A. Scorzoni, B. Neri, C. Caprile, and F. Fantini, Mater. Sci. Rep. **7**, 143 (1991).
[3]T. Kwok, P. S. Ho, and H.-C. W. Huang, J. Vac. Sci. Technol. A **2**, 241 (1984).
[4]A. J. Patrinos and J. A. Schwarz, Thin Solid Films **196**, 47 (1991).
[5]L. Berenbaum and R. Rosenberg, Thin Solid Films **4**, 187 (1969).
[6]A. Blech and E. S. Meieran, Appl. Phys. Lett. **11**, 263 (1967).
[7]M. Paniccia, P. Flinn, and R. Reifenberger (private communication).
[8]G. L. Baldini and A. Scorzoni, Thin Solid Films **191**, 31 (1990).
[9]A. Diligenti, P. E. Bagnoli, B. Neri, S. Brea, and L. Mantellassi, Solid-State Electron. **32**, 11 (1989).
[10]G. Reiss, L. E. Levine, and D. A. Smith, J. Vac. Sci. Technol. B **11**, 108 (1993).
[11]P. Muralt and D. W. Pohl, Appl. Phys. Lett. **48**, 514 (1986).
[12]A. D. Kent, I. Maggio-Aprile, Ph. Niedermann, Ch. Renner, and Ø. Fischer, J. Vac. Sci. Technol. A **8**, 459 (1990).
[13]S. Buchholz, H. Fuchs, and J. P. Rabe, J. Vac. Sci. Technol. B **9**, 857 (1991).
[14]G. Reiss and L. E. Levine (unpublished).
[15]L. E. Levine, G. Reiss, and D. A. Smith (unpublished).
[16]H. B. Huntington, Thin Solid Films **25**, 265 (1975).
[17]K. N. Tu, Phys. Rev. B **45**, 1409 (1992).

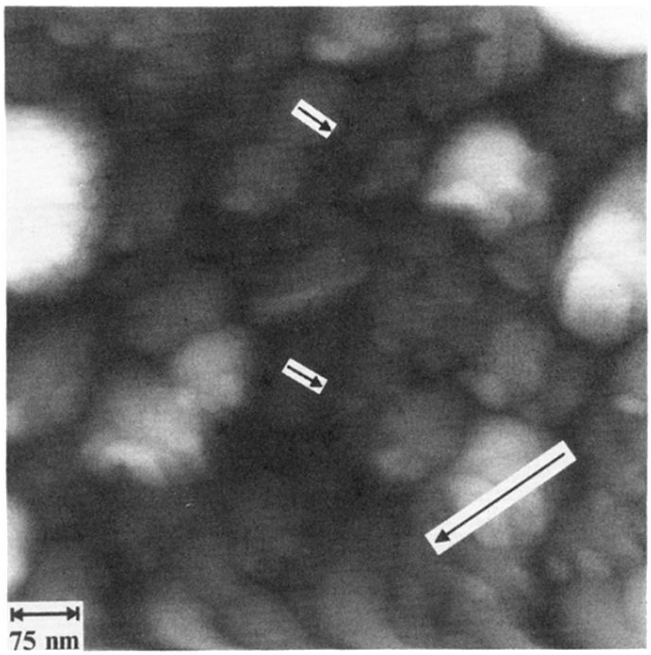

FIG. 3. Topographic STM scan of a Ag film carrying a dc current of 1.4×10^4 A/cm^2. The range of the height distribution for the scan is 300 Å (black-white). The small arrows indicate representative small nodules at divergence points and the large arrow points in the direction of the electron flux.

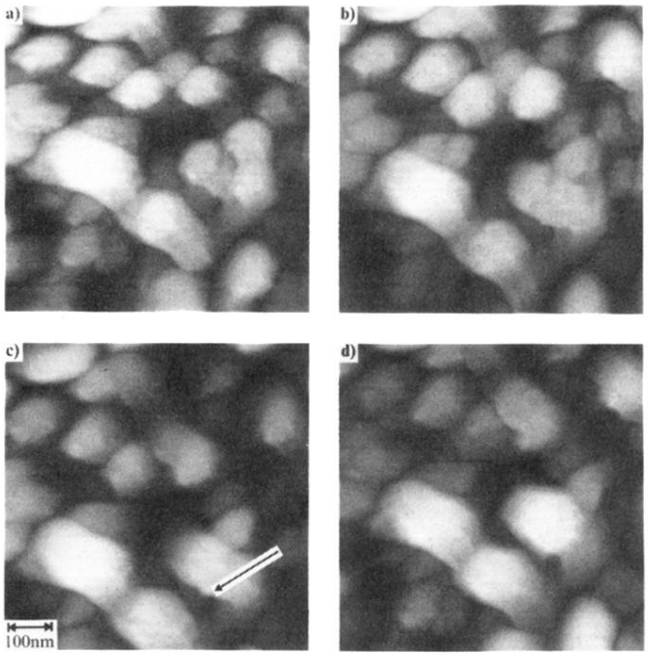

FIG. 7. Four topographic STM scans from the same area of the sample at different times and current densities as described in the text. The range for the height scale is 360 Å and the arrow points in the direction of the current flow. The structural changes suggest a grain growth mechanism driven by current transport.